Supplementary Figures and Legends

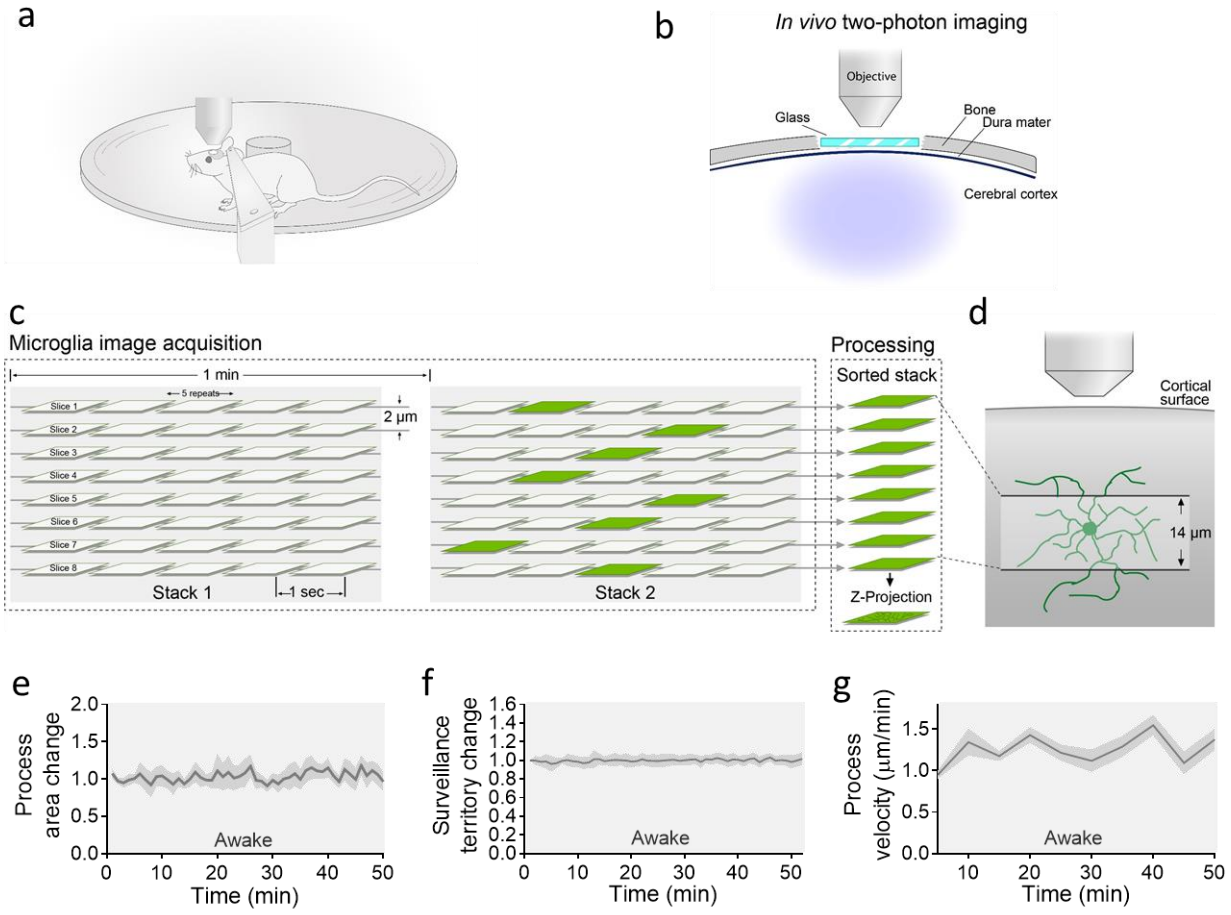

Supplementary Figure 1. *In vivo* imaging of microglia in awake mice.

a, The circular treadmill system and head restraint for mice. **b**, Imaging of chronic, glass cranial windows. **c**, Microglial image acquisition and processing method for awake mice. Of the five replicates, green frames represent the frame chosen by the user at each z level which shows the least distortion in the x/y plane due to movement. These frames are then assembled into a z-stack and aligned before obtaining a maximal z-projection image. **d**, All microglia with a soma near the middle of the Z stack and processes fully incorporated in the x/y plane were used in analyses. **e-f**, Time lapse imaging in awake mice over a 50 min period indicate relatively stable process area and surveillance territories are maintained over time. **g**, Microglial process velocity follows relatively cyclical patterns when assessed over 5 min epochs. Trend lines display the mean ± SEM change in (**e-g**), *n*=9 cells/3 mice.

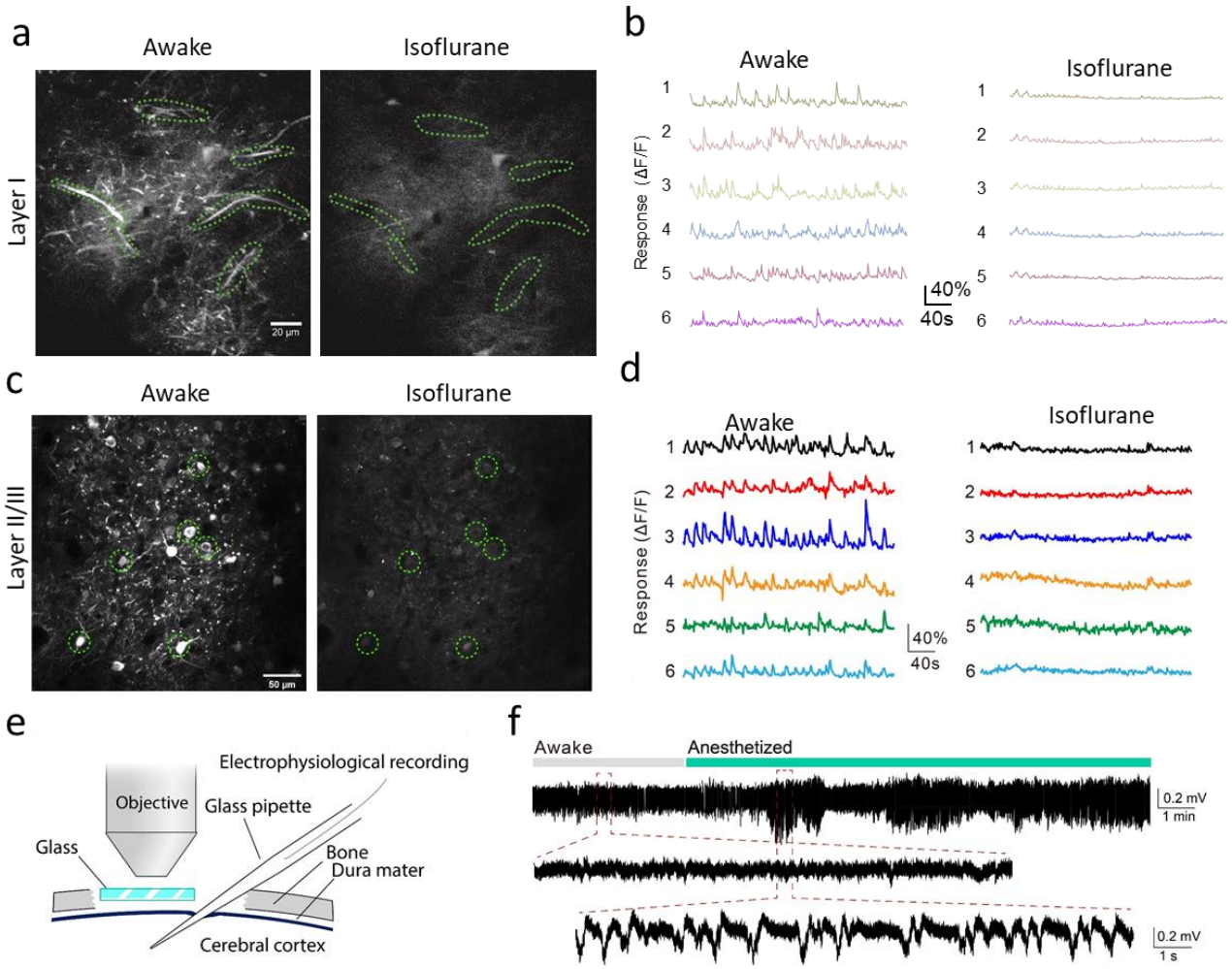

Supplementary Figure 2. Neuronal network activity in the somatosensory cortex of awake and anesthetized mice.

a,**c**, Two-photon imaging of neuronal calcium activity in the layer 1 dendrites (**a**) and layer 2/3 somas (**c**) of excitatory neurons, labelled by AAV9.CamKII.GCaMP6s.WPRE.SV40. Maximum intensity projections of calcium activity are shown just before and 1 min after isoflurane anesthesia (3% initiation; 1.2% maintenance). **b**, ΔF/F traces from six representative dendrites outlined in (**a**) before and 1 min after isoflurane anesthesia. **d**, ΔF/F traces from six representative somas circled in (**c**) before and 1 min after anesthesia. **e**,**f**, Field potential recordings 50 µm beneath the cortical surface showing slow wave activity emerging after isoflurane anesthesia. All experiments were repeated three times independently with similar results.

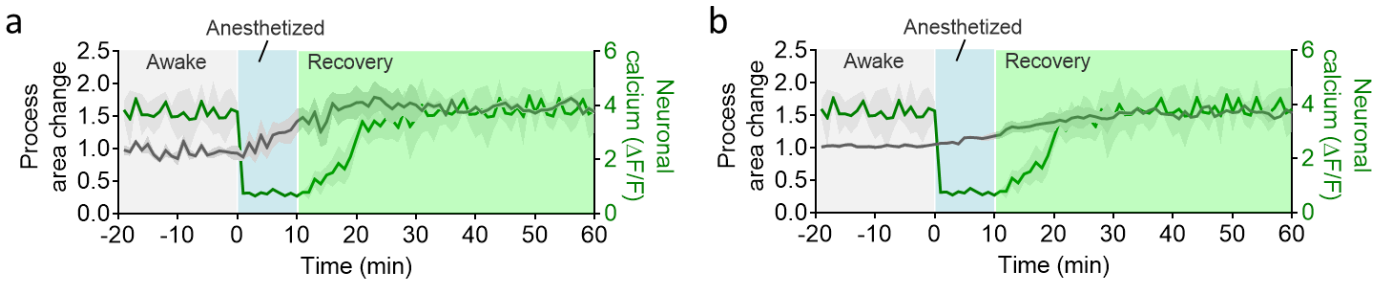

Supplementary Figure 3. Transient anesthesia triggers prolonged microglial surveillance increases

Time-lapse changes of microglial process area (**a**) and surveillance territory (**b**) in the awake, anesthetized (isoflurane, 10 min), and recovering when isoflurane anesthesia is removed. Corresponding neuronal calcium activity is overlaid with microglial process metrics during these periods. Trend lines display the mean ± SEM change, *n*=9 cells/3 mice.

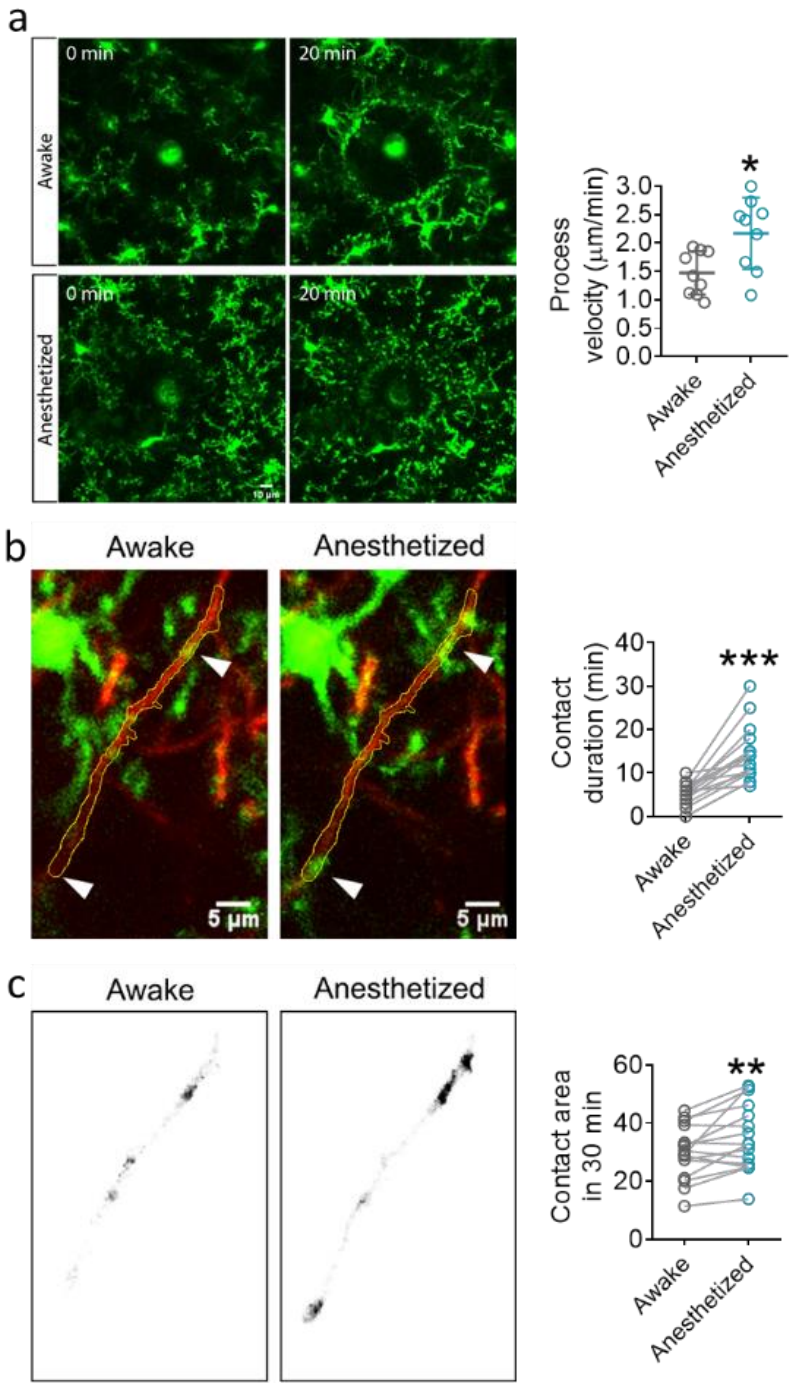

Supplementary Figure 4. Microglial processes response to laser burn and interaction with neuronal dendrite in awake and anesthetized conditions.

a, Two-photon, time-lapse imaging of microglial processes responding to laser burn in awake and anesthetized conditions. Processes velocity was greater in the anesthetized condition compared to the awake condition (Awake: 1.473±0.128; Anesthetized:

2.169±0.209; *P*=0.012, t(16)=2.835, *n*=9 events/3 mice for each group, **P*<0.05, unpaired t-test (two-tailed)). **b**, Two-photon imaging of microglial processes and neuronal dendrites in awake and anesthetized conditions. The contact duration was longer under anesthetized conditions compared to the awake condition (*P*<0.0001, t(15)=6.311). **c**, The overlapping area (black) between processes and a dendrite (yellow line in **b**) was quantified as contact area (left). This area was normalized over 30 min to the contact area in the first 10 min under the awake condition (*P*=0.0089, t(15)=3.005). *N*=16 fields/3 mice for each group in (**b**,**c**), ***P*<0.01, *** *P*<0.001, paired t-test (two-tailed).

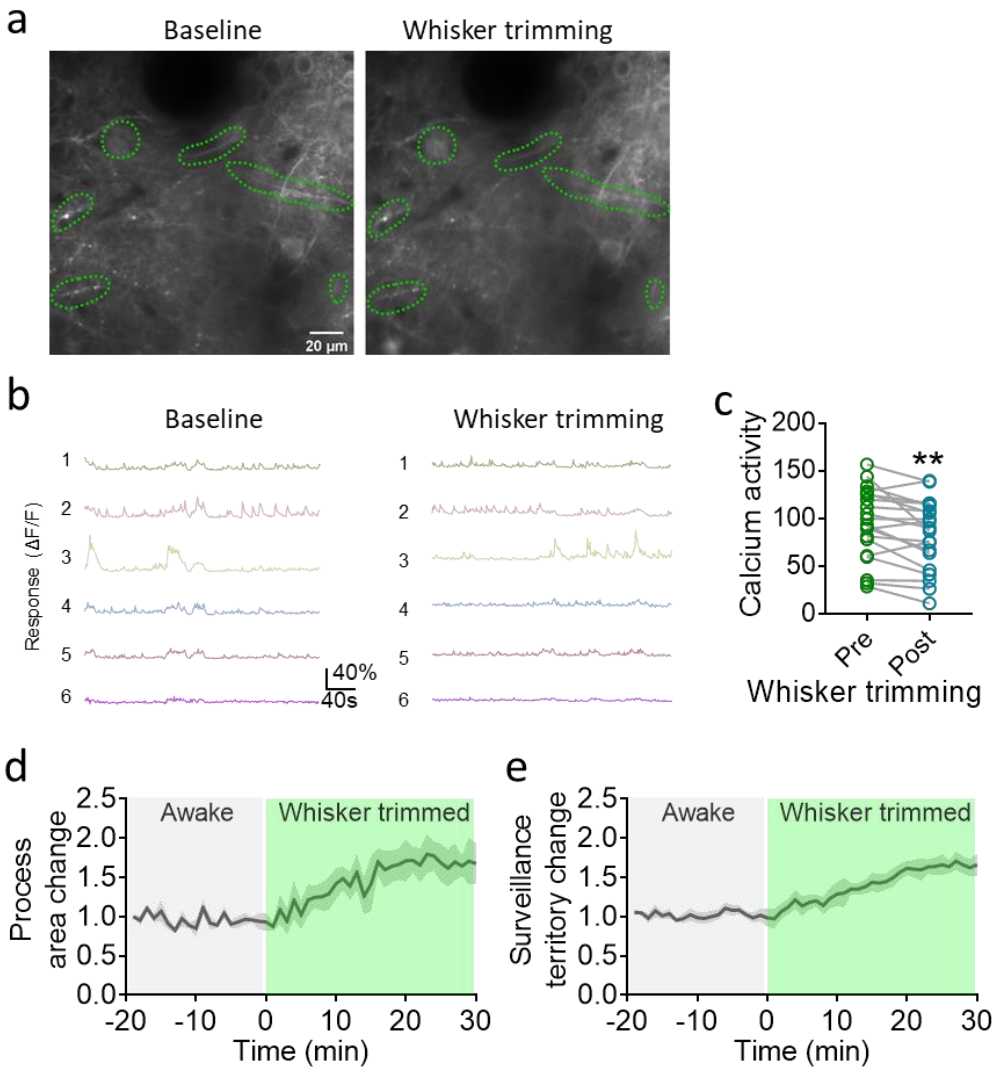

Supplementary Figure 5. Neuronal network activity decreases and microglial surveillance increases after whisker trimming.

a, Two-photon, time-lapse imaging of neuronal dendrite calcium activity (50 µm depth) before and after contralateral whisker trimming. **b**, ΔF/F traces from six representative neuronal dendrites (outlined in **a**) prior to and after whisker trimming. **c**, Sum of ΔF/F calcium activity (threshold: ΔF/F >0.2) 5 min before and after whisker trimming (*P*=0.0035, t(8)=3.333). *N*=20 clearly observable dendrites/3 mice which were randomly selected and analyzed, ***P*<0.01, paired t-test (two-tailed). **d**-**e,** Time-lapse changes in microglial process area (**d**) and surveillance territory (**e**) in awake mice before and after whisker trimming. Trend lines display the mean ± SEM change, *n*=9 cells/3 mice. Experiments were repeated three times independently with similar results in (**a**,**b**).

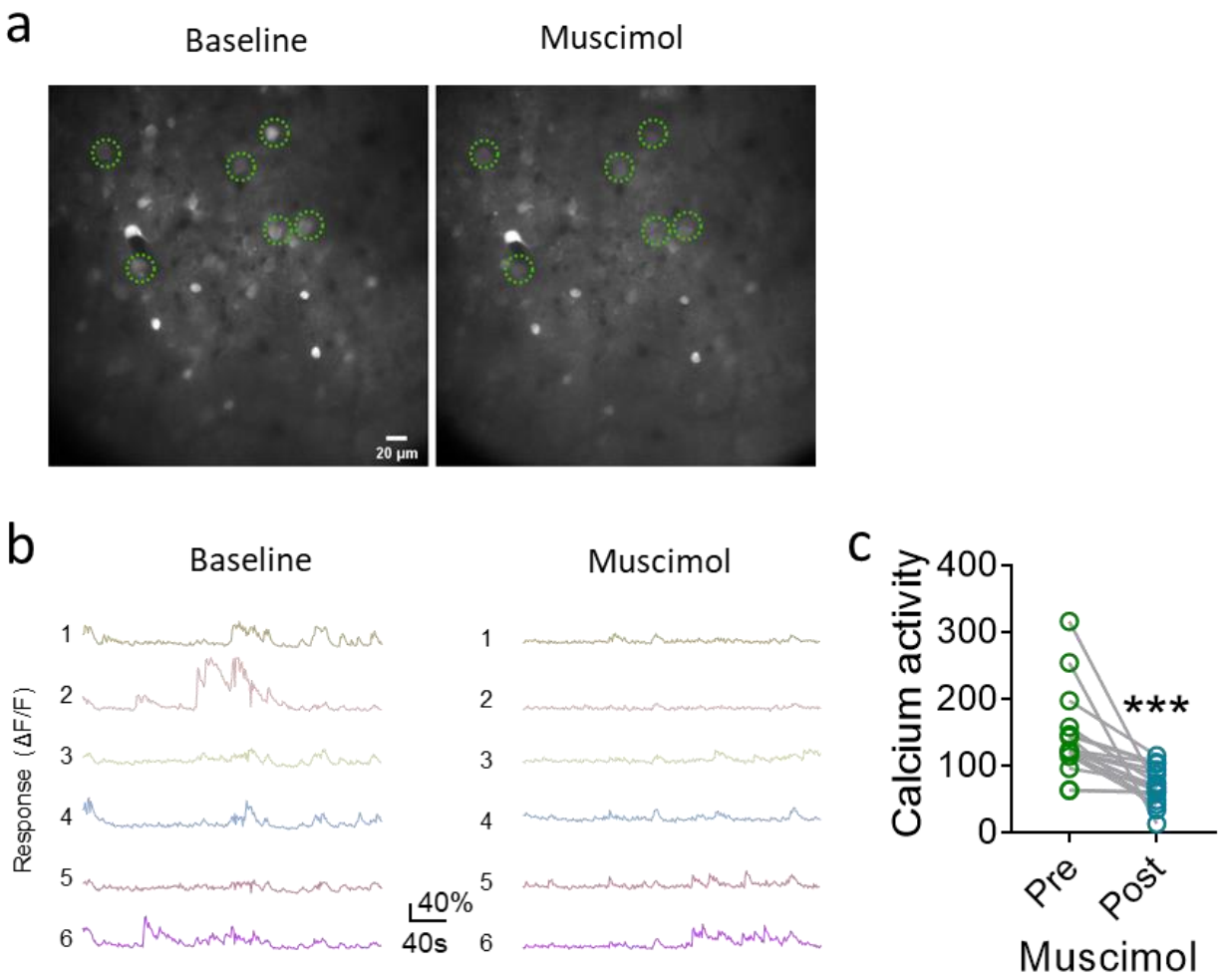

Supplementary Figure 6. Neuronal network activity decreases after muscimol application.

a, Two-photon, time-lapse imaging of somatic calcium activity from layer 2/3 excitatory neurons (150 μm depth) before and after intracerebral administration of muscimol (870 μM, 10 μL). **b**, ΔF/F traces from six representative somas (circles in **a**) before and after muscimol application. **c**, Sum of ΔF/F calcium activity (threshold: ΔF/F >0.2) 5 min before and after muscimol application (P=0.0005, t(8)=4.303). N=18 clearly observable dendrites/3 mice which were randomly selected and analyzed, ***P<0.01, paired t-test (two-tailed). Experiments were repeated three times independently with similar results in (**a**,**b**).

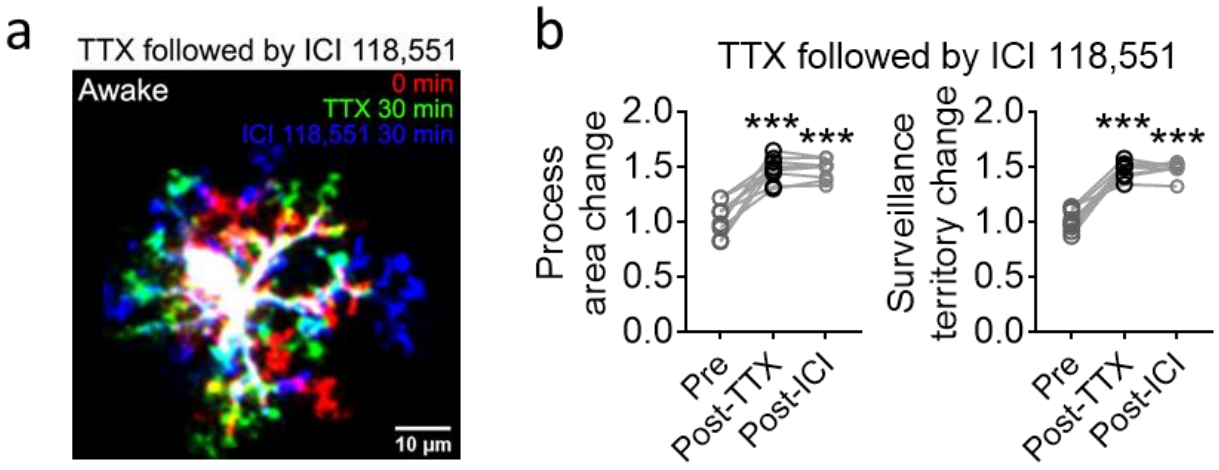

Supplementary Figure 7. Intracerebral application of TTX increases microglial process surveillance.

a, Microglial morphology in awake mice at three time points: 0 min (red) and 30 min (green) after TTX (10 µM) application, and another 30 min (blue) after ICI 118,551 (30 µM, 10 µL) administration. **b**, Microglial process area and surveillance increase 30 min after TTX but do not show an additional increase when ICI 118,551 is later administered (area: Post-TTX vs Pre, P=0.0004, t(8)=6.765; Post-ICI vs Pre, P=0.0004, t(8)=6.939; Post-TTX vs Post-ICI, P=0.851, t(8)=0.194; territory: Post-TTX vs Pre, P<0.0001, t(8)=11.06; Post-ICI vs Pre, P<0.0001, t(8)=10.07; Post-TTX vs Post-ICI, P=0.472, t(8)=0.756). N=9 cells/3 mice each group, ***P<0.001, one-way ANOVA. Experiments were repeated three times independently with similar results in (**a**).

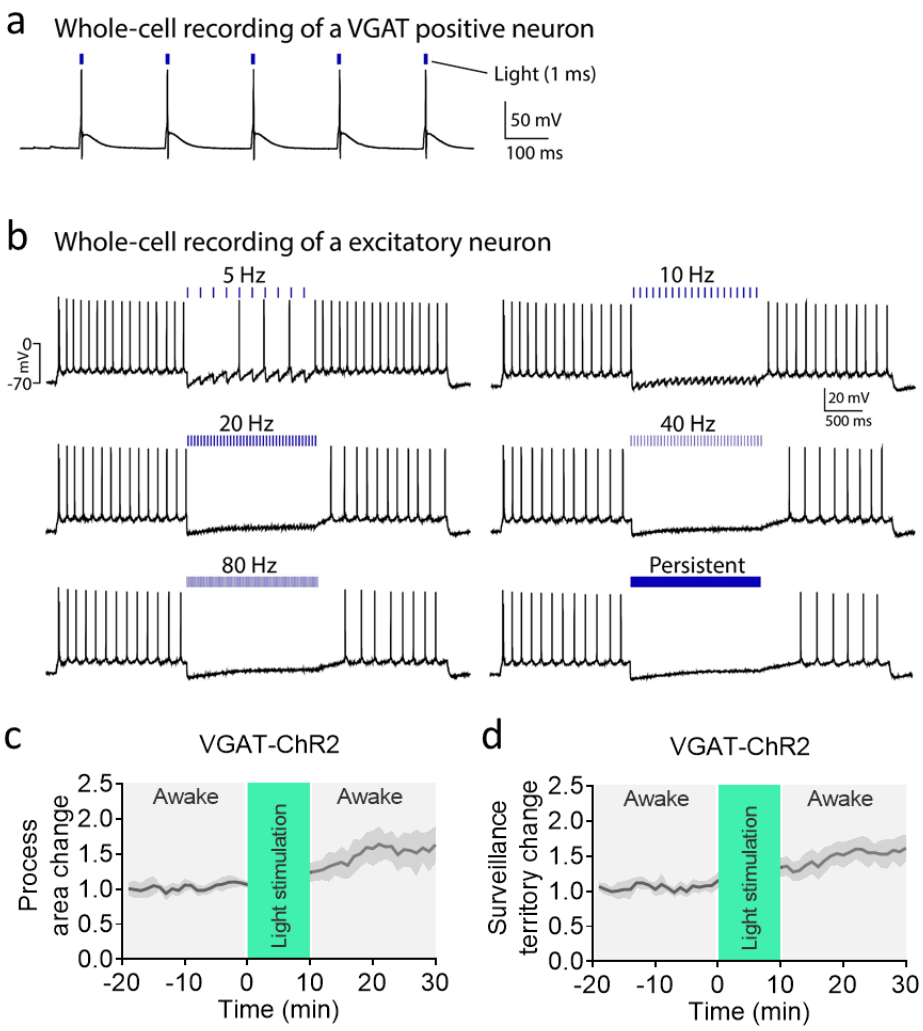

Supplementary Figure 8. Verification of channelrhodopsin-2 function in VGAT-positive neurons and effects on local excitatory neurons.

a, Whole-cell recording from a VGAT-positive inhibitory interneuron expressing ChR2 and membrane potential changes in response to 1 ms blue light pulses. **b**, Whole-cell recording from putative excitatory pyramidal neurons near a labelled VGAT-ChR2 cell(s). In putative excitatory neurons, increasing frequencies of optogenetic stimulation to nearby VGAT-ChR2 cells results in a distinct suppression of firing activity. Above results were replicated in 3 mice. **c**, **d**, Time-lapse changes in microglial process area (**c**) and surveillance territory (**d**) in the VGAT-ChR2 mice before and after 10 min blue light stimulation (1 ms, 10 Hz, 10min, 470 nm) as indicated. Trend lines display the mean ± SEM change, *n*=9 cells/3 mice. Experiments were repeated three times independently with similar results in (**a**,**b**).

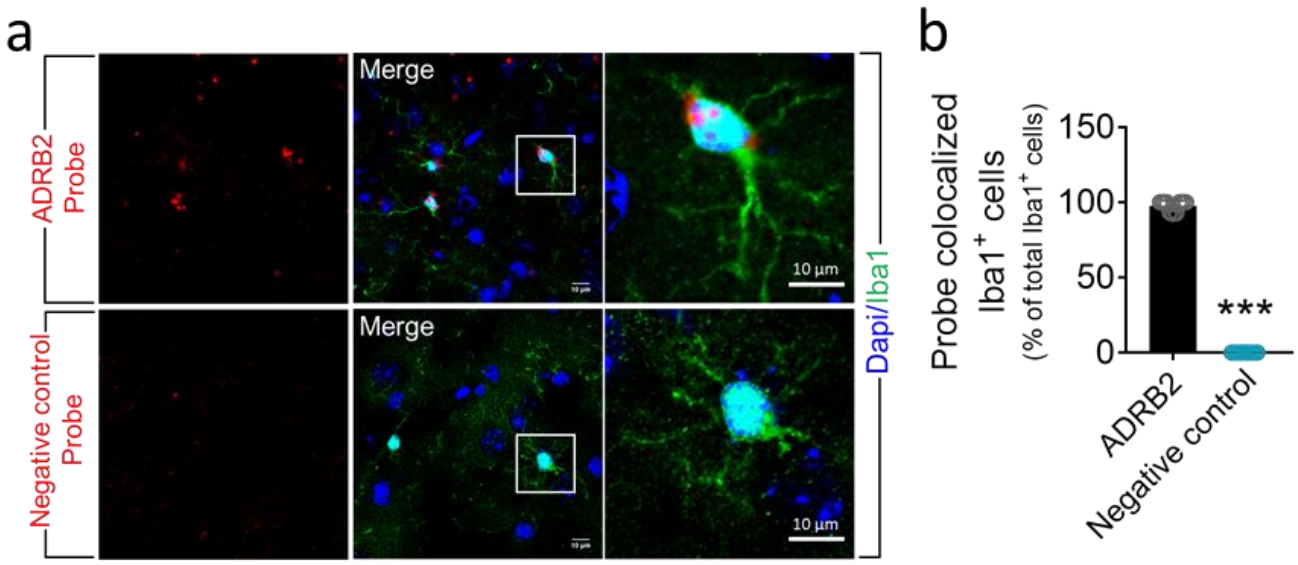

Supplementary Figure 9. β2-adrenergic receptor (ADRB2) mRNA is enriched in microglia

a, RNAscope *in situ* hybridization analysis of ADRB2 mRNA in the somatosensory cortex. Red: ADRB2 or negative control probe; green: Iba1; blue: Dapi. **b**, Quantification of probes colocalized to Iba1 positive cells (ADRB2: 97.6%±0.012; Negative control: 0%; $P<0.0001$, $t(16)=81.14$). $N=9$ fields of view/3 mice each group, ***$P<0.001$, unpaired t-test (two-tailed). Experiment was repeated three times independently with similar results in (**a**).

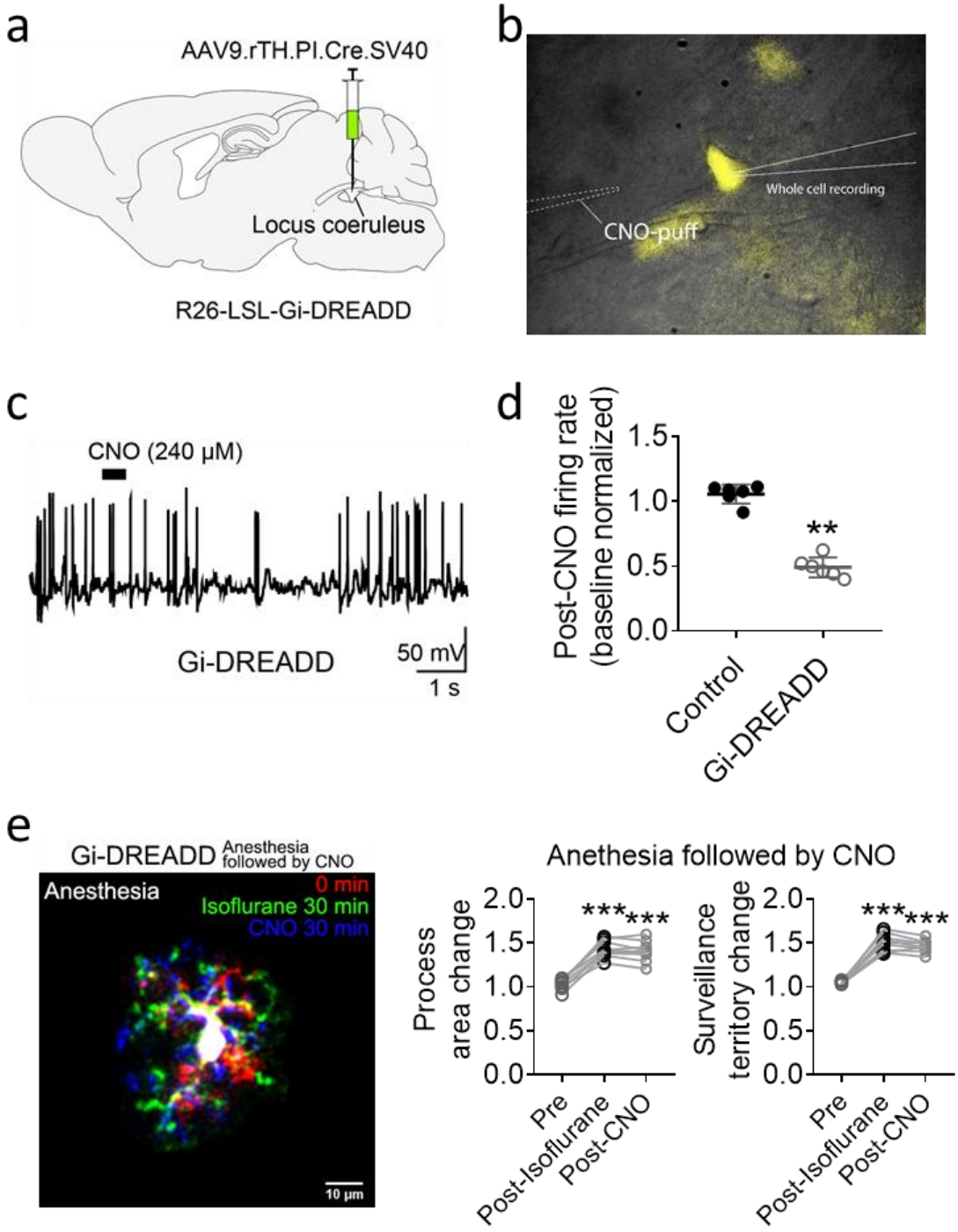

Supplementary Figure 10. Noradrenergic neurons of the locus coeruleus are inhibited by CNO application in Gi-DREADD mice

a, An adeno-associated virus, driving Cre recombinase expression under the tyrosine hydroxylase (rTH) promoter (AAV9.rTH.Cre), was injected in the locus coeruleus (LC) of

Gi-DREADD mice and their control littermates that did not express the Gi-DREADD transgene. **b**, Representative recording of a Gi-DREADD expressing noradrenergic neuron and application of clozapine N-oxide (CNO) by puffing through a glass pipette. **c**, Representative whole-cell recording from the experiment shown in (**b**). After a delay associated with CNO diffusion, Gi-DREADD neurons in the LC display a marked reduction in firing frequency. **d**, Effects of CNO on firing rate are only observed in Gi-DREADD transgenic animals, and not in non-transgenic sibling littermates (Control: 1.058±0.030; Gi-DREADD: 0.4925±0.032; P=0.002, t(10)=12.9; n=6 cells/3 mice for each group, **P<0.01, unpaired t-test (two-tailed)). **e**, Microglial morphology in Gi-DREADD mice at three time points: 0 min (red) and 30 min (green) after anesthesia, and another 30 min (blue) after CNO (5 mg/kg, i.p.) administration (left). Microglial process area and surveillance increase 30 min after anesthesia but do not show an additional increase when CNO is later administrated (area: Post-Isoflurane vs Pre, P<0.0001, t(8)=13.9; Post-CNO vs Pre, P<0.0001, t(8)=11.28; Post-Isoflurane vs Post-CNO, P=0.624, t(8)=1.374; territory: Post-Isoflurane vs Pre, P<0.0001, t(8)=13.86; Post-CNO vs Pre, P<0.0001, t(8)=17.45; Post-Isoflurane vs Post-CNO, P=0.2919, t(8)=2.038). N=9 cells/3 mice for each group, ***P<0.001, one-way ANOVA. Experiments were repeated three times independently with similar results in (**b**,**c**,**e**).

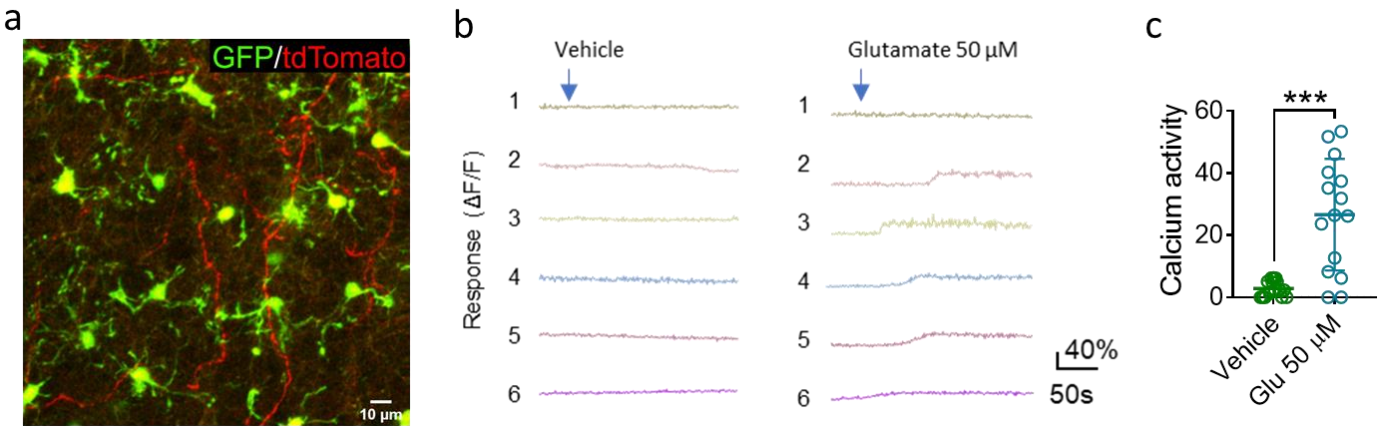

Supplementary Figure 11. Microglial process surveillance and neuronal network activity in acute brain slices

a, The fluorescent micrograph shows that LC projections (tdTomato label) in the somatosensory cortex are preserved in transverse acute brain slices. **b**, ΔF/F traces from six representative neurons of somatosensory cortex in acute brain slices before and after 50 µM glutamate bath administration. **c**, Sum of ΔF/F calcium activity (threshold: ΔF/F >0.2) over 5 min before and after glutamate bath application (Vehicle: 2.799±0.658; Glu 50 µM: 26.63±4.634; P<0.0001, t(28)=5.091). N=15 somas/3 mice each condition, ***P<0.001, unpaired t-test (two-tailed). Experiments were repeated three times independently with similar results in (**a**,**b**).

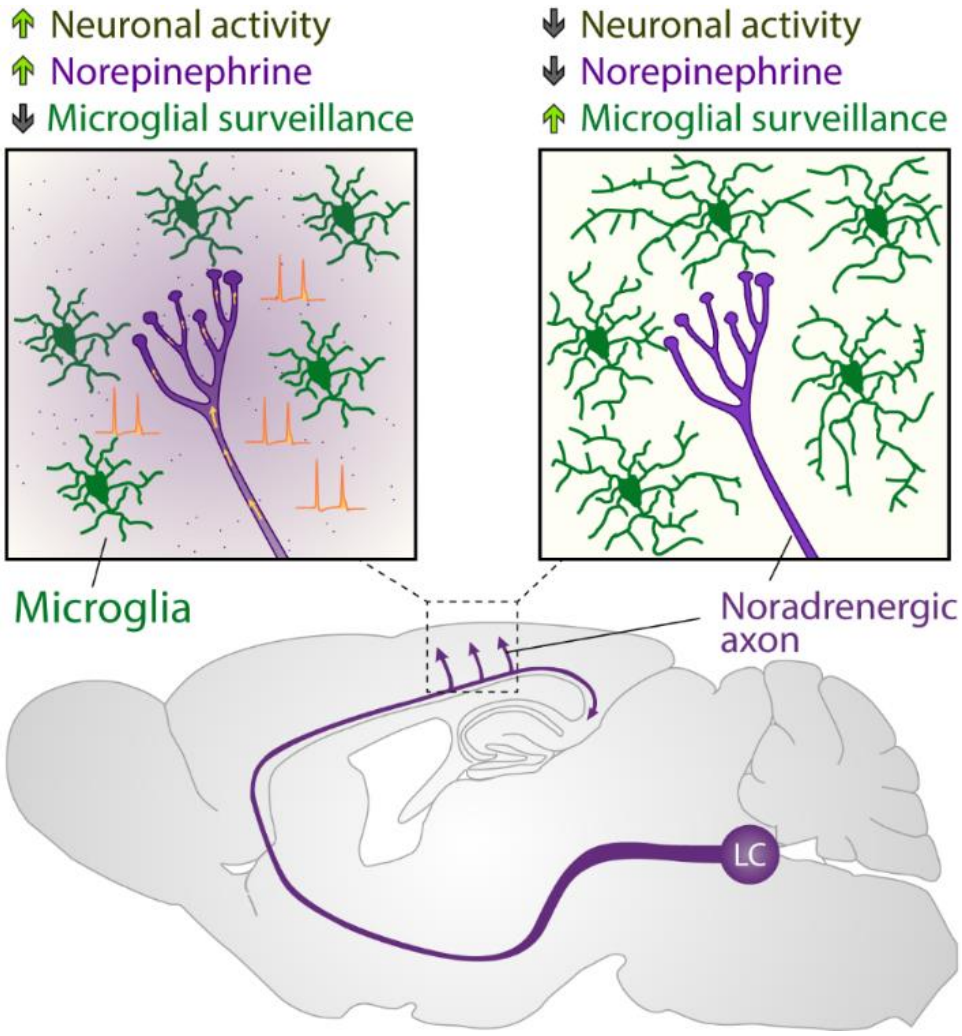

Supplementary Figure 12. Schematic diagram for norepinephrine-dependent changes in microglial process surveillance territory

In awake mice, high NE tone (purple) limits microglial process dynamics, characterized by reduced process area, velocity, and territory of surveillance. However, when neuronal activity is suppressed (general anesthesia, sensory deprivation, or increased network inhibition), a corresponding reduction in NE tone triggers increased microglial processes surveillance. The proposed mechanism suggests that NE levels in the awake brain serve as an overriding signal restraining microglial process dynamics.